

THE GIANT DIPOLE RESONANCE AS A PROBE OF NUCLEAR STRUCTURE UNDER EXTREME CONDITIONS*

M. DI TORO^a, V. BARAN^b, M. CABIBBO^a, M. COLONNA^a
A.B. LARIONOV^c, S. MACCARONE^a AND N. TSONEVA^d

^aLNS-INFN and Phys.Dept. University of Catania
44 Via S.Sofia, 95123 Catania, Italy

^bNIPNE Bucharest Romania

^cKurchatov Inst. Moscow, Russia

^dINRNE Sofia, Bulgaria

(Received August 11, 1998)

We investigate the properties of the Giant Dipole Resonance (GDR) built on very exotic nuclear systems: *(i)* High temperature, at the limit of nuclear stability. We discuss first the problem of hot nuclei formation then we analyse the possibility of observation of a zero- to first sound transition for the dipole propagation. *(ii)* Shape and charge equilibration in fusion dynamics. We describe the features of direct GDR photon emissions from intermediate dinuclear systems with very exotic shapes or charge distributions formed in particular entrance channels (mass symmetry vs. charge symmetry). *(iii)* Isospin. We show the effect of large charge asymmetry on propagation of isovector modes. Mixing to isoscalar components and possible new instabilities are predicted, related to the structure of the symmetry term of effective interactions.

PACS numbers: 24.10.-i, 24.30.Cz

1. Introduction

The isovector giant dipole resonance represents a well established collective motion of finite nuclei extensively studied since more than fifty years [1]. The dependence on the nuclear structure of the reference state on top of which the collective mode is built has already suggested its application in order to study nuclei far from the ground state. The time structure of the

* Presented at the International Conference "Nuclear Physics Close to the Barrier", Warszawa, Poland, June 30–July 4, 1998.

GDR mode actually allows a possibility of using it as a probe of nuclear systems very far from normal conditions.

We can roughly estimate an oscillation period of $\hbar/E_{\text{GDR}} \simeq 10\text{--}20 \text{ fm}/c$ and a mean life-time $\hbar/\Gamma_{\text{GDR}} \simeq 50 \text{ fm}/c$. Since the spreading width is the largest contribution to the total width Γ_{GDR} we can estimate around $50 \text{ fm}/c$ also the time needed to build up the collective GDR mode in a Compound Nucleus (C.N.). All these time scales are relatively short and this makes the GDR an ideal probe to study nuclear systems under extreme conditions.

In this report we will first analyse temperature effects. Using a simple estimation for neutron evaporation with the Weisskopf formula [2] we can estimate a mean lifetime for heated compound nuclei going from $10^5 \text{ fm}/c$ at $T = 1 \text{ MeV}$ to $50 \text{ fm}/c$ at $T = 5 \text{ MeV}$, so it seems possible to follow some GDR emission up to the stability limits of a hot C.N. This will be the subject of the Sect. 2 where we will discuss first the problems of hot nuclei formation and then the temperature dependence of the GDR damping.

In fusion dynamics we expect to have entrance channel effects associated to time scales that allow the use of GDR emissions to study properties of very exotic dinuclear systems, see Sect. 3. For mass-symmetric channels we have shape equilibration times that can reach some units in $10^3 \text{ fm}/c$, then we can have the chance of detecting GDR photons emitted in this time interval with characteristic features of the path to fusion. Charge equilibration takes place on time scales of few units in $10^2 \text{ fm}/c$: in charge asymmetric entrance channels we expect to see a “direct dipole” emission, again with special dynamical features, which should give an extra yield to the photon spectrum in the GDR region.

Finally in Sect. 4 the GDR structure in very asymmetric beta-unstable nuclei will be discussed in the general framework of dispersion relations for collective modes in asymmetric nuclear matter. A strong coupling to isoscalar components and new instabilities are expected. A possibility of extracting new information on the symmetry term of the nuclear Equation of State (EOS) is also analysed.

Some perspectives are presented in Sect. 5.

2. GDR in hot nuclei

The GDR γ -emission has been extensively used to study the structure of excited nuclei, see the nice reviews [3, 4]. With increasing excitation energy the experimental results are, however, quite controversial, in particular on the temperature dependence of the GDR damping mechanisms, and so the evaluation of a limit temperature for the disappearing of the isovector dipole mode is still an open problem. Uncertainties in the data analysis are mostly coming from:

- (i) Hot nuclei formation (pre-equilibrium dynamical effects) [5, 6];
- (ii) Statistical CASCADE calculations [7];
- (iii) Subtraction of a direct bremsstrahlung component [8].

The point (i) is particularly delicate. The saturation of the GDR photon yield, observed in all experiments [9], can be indeed related to dynamical limits in thermal energy deposition on the detected heavy residue and not to a reduction of the GDR strength in hot nuclei. These pre-equilibrium effects seem to represent a serious intrinsic limitation to the use of fusion reactions to form hot nuclei. Inelastic α scattering experiments have given very nice data on heated nuclei, with smaller pre-equilibrium bias and less angular momentum effects [10, 11]. There is, however, an intrinsic limit on the excitation energy reached. New ways to form hot nuclei should be pursued.

Inelastic α scattering results clearly show a quite fast increase of the GDR damping with temperature in medium heavy and heavy nuclei (Sn, Pb). Two models, one based the collisional damping and the other on shape fluctuations in an adiabatic picture, can reproduce this trend, see [7]. The point we would like to stress here is that at $T \simeq 3$ MeV the width appears of the same order as the centroid energy and so we expect a disappearing of the GDR signal.

Recently the possibility of a transition from zero to first sound for the Giant Dipole propagation in hot nuclei has been suggested in order to allow a collective GDR emission from very excited nuclei [6, 12, 13]. This transition has been already clearly observed in other Fermi liquids, like ^3He [14].

Zero sound modes are mean field oscillations, quantum collective vibrations of the Fermi surface [15–17] while first sounds manifest as hydrodynamical waves. The damping mechanisms in the two regimes are quite different: mean field oscillations are relaxed by two-body collisions, collective modes due to local pressure variations by single particle escape from the flow. Consequently the temperature behaviour of the spreading width in Fermi liquids is just the opposite in the two cases: proportional to T^2 for zero sounds and to $1/T^2$, *i.e.* following the mean free path, for first sounds. In case of a transition the expected saturation and eventual decrease of the attenuation could be the right mechanism to allow the GDR observation up to very high temperatures.

We remark that the possibility of such transition in hot nuclear systems has been recently suggested also for the fission mode [18–20].

We show some predictions of a dispersion relation approach [15, 16, 21, 22] extended to isovector modes. This is correct in order to study the nuclear matter response, *i.e.* to describe volume dipole modes of Steinwedel–Jensen

(SJ) type. We insert finite nucleus effects just rescaling the wavelength of the normal modes. We expect this picture to have good physical grounds with increasing temperature due to the melting of shell effects and to the shorter nucleon mean free path which strongly reduces surface effects.

We find that the zero to first sound transition for isovector modes has quite relevant new features due to the presence of a counter streaming flow between neutrons and protons, absent in other “one component” Fermi liquids. As a consequence the effect of the transition on sound velocity and damping appears less dramatic but none the less still observable in the emitted photon spectra.

The starting point is the linearized kinetic equation for the variation of the isovector distribution function $\delta f_i = \delta f_p - \delta f_n$ taking into account the effect of collisions in a relaxation time approximation:

$$\frac{\partial \delta f_i}{\partial t} + \frac{\mathbf{p}}{m} \frac{\partial \delta f_i}{\partial \mathbf{r}} - \frac{\partial(\delta U_p - \delta U_n)}{\partial \mathbf{r}} \frac{\partial f^{(0)}}{\partial \mathbf{p}} = -\frac{(\delta f_i)_{l=1}}{\tau_1} - \frac{(\delta f_i)_{l \geq 2}}{\tau_2}, \quad (1)$$

where the superscript (0) labels stationary values and δU_q is the dynamical component of the mean field potential. The unperturbed distribution function $f^{(0)}$ is in general the Fermi distribution at finite temperature. As self-consistent mean field potential we use a Skyrme-like form :

$$U_q = A \left(\frac{\rho}{\rho_0} \right) + B \left(\frac{\rho}{\rho_0} \right)^{\alpha+1} + C \left(\frac{\rho'}{\rho_0} \right) \tau_q, \quad (2)$$

where $\rho = \rho_n + \rho_p$ and $\rho' = \rho_n - \rho_p$ are respectively the total (isoscalar) and the relative (isovector) density; $\rho_0 = 0.16 \text{ fm}^{-3}$ is the nuclear saturation density; $\tau_q = +1$ ($q = n$), -1 ($q = p$). The values of the parameters $A = -356.8 \text{ MeV}$, $B = 303.9 \text{ MeV}$, $\alpha = 1/6$ are adjusted to reproduce the saturation properties of symmetric nuclear matter, with a compressibility modulus $K = 201 \text{ MeV}$. At saturation density the potential symmetry energy coefficient $C(\rho_0) = 32 \text{ MeV}$ satisfies the condition [22]:

$$a_{\text{sym}} = \frac{\varepsilon_F}{3} + \frac{C(\rho_0)}{2},$$

where $a_{\text{sym}} = 28 \text{ MeV}$ is the symmetry energy coefficient in the Weizsäcker mass formula and $\varepsilon_F = 36 \text{ MeV}$ is the Fermi energy for symmetric nuclear matter at $\rho = \rho_0$.

On the right side of Eq. (1) $(\delta f_i)_l$ are distortions of the local isovector d.f. having multipolarity l . We consider a generalization of relaxation time method. In the case of isoscalar motion, when protons and neutrons are moving in phase, the conservation laws for particle number, momentum and

energy will impose only multipoles $l \geq 2$. However, in the case of out of phase motion the effect of collisions is also to damp the isovector current, a process characterized by a relaxation time τ_1 . The relaxation of higher order multipoles is associated to an effective relaxation time τ_2 . Following a standard procedure as described in [16,23], one can derive from Eqs (1) a generalized dispersion relation for isovector sound in a two-component Fermi liquid:

$$\left(1 + \frac{1}{\xi_2 \sigma_2}\right) - w(\xi_2) \left\{ \left(F'_0 - \frac{1}{\xi_2 \sigma_2}\right) - 3\xi_2 \left(\frac{1}{\sigma_2} - \frac{1}{\sigma_1}\right) \left(1 + \frac{1}{\xi_2 \sigma_2}\right) \right\} = 0, \tag{3}$$

where

$$\xi_2 = \frac{i\omega\tau_2 - 1}{i\tau_2 k v_F}, \quad \sigma_1 = i\tau_1 k v_F, \quad \sigma_2 = i\tau_2 k v_F \tag{4}$$

$w(\xi_2)$ is the Lindhard function

$$w(\xi_2) = \frac{1}{2}\xi_2 \ln \frac{\xi_2 + 1}{\xi_2 - 1} - 1 \tag{5}$$

and F'_0 is the isovector Landau parameter depending on symmetry potential energy coefficient C : $F'_0 = 3C/(2\varepsilon_F) = 1.33$.

The generalized dispersion relation Eq. (3) connects real and imaginary parts of eigenfrequencies to the Landau parameter and the two relaxation times. It is useful to analyze two analytical limiting cases from where we get some insight regarding zero and first isovector sounds: (a) zero sound limit, $\omega_r \tau_2 \gg 1$; (b) first sound limit, $\omega_r \tau_2 \ll 1$ [26]. The relative temperature dependence of centroids and widths are reported in figures 1, 2 for the Pb case.

The correct way to compare theoretical predictions with experiments is to compute GDR strength functions at various temperatures to insert in statistical cascade analyses [7]. In this scheme we can also get centroid energies and FWHM (Full Width Half Maximum) that already will give some indications. From Eq. (1) we can derive the isovector collective response function [24] and then the dipole strength function $S_k(\omega)$ following a standard approach (see Refs [21, 25, 26]). The photoabsorption cross section by a thermally excited nucleus, to be used in cascade calculations, can be expressed in terms of the strength function as follows [21,25]:

$$\sigma_{abs}(\hbar\omega) = \frac{4\pi^2 e^2}{\hbar c k^2 \rho_0} \frac{NZ}{A} \hbar\omega S_k(\omega). \tag{6}$$

In the following we will compare predictions for the temperature behaviour of GDR strength functions in ^{208}Pb ($k = \pi/2R_{\text{Pb}} = 0.22 \text{ fm}^{-1}$).

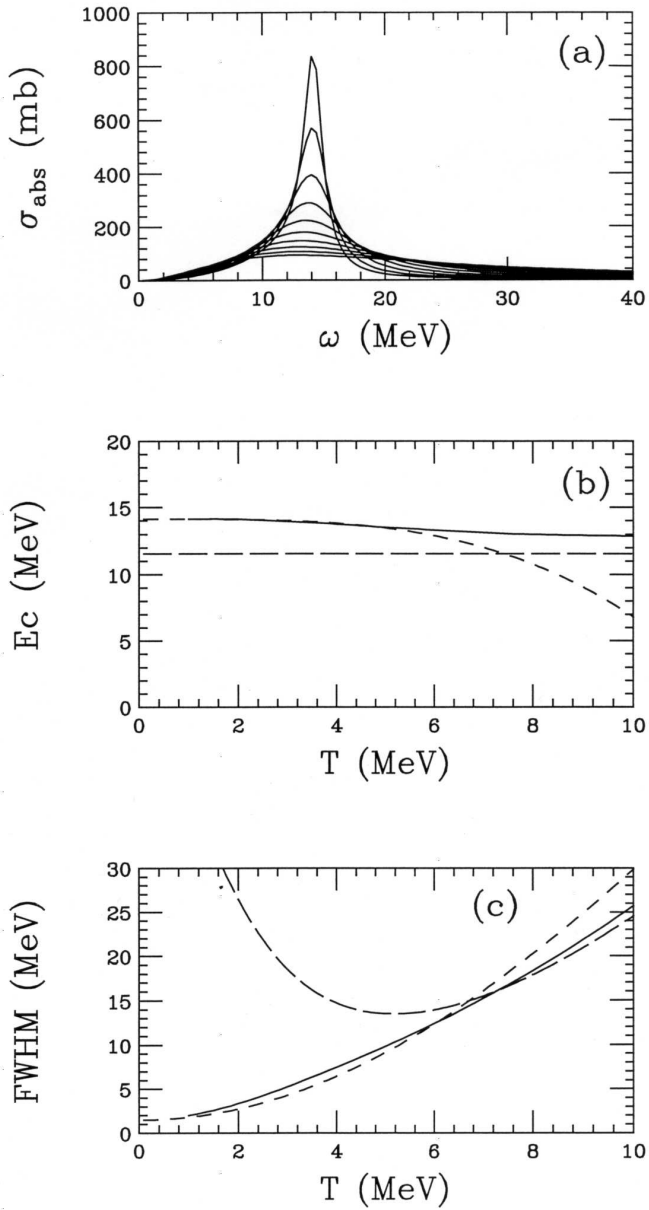


Fig. 1. Temperature dependence of Pb GDR strength distributions for $\tau_2 = \tau_1$. (a) — complete calculation of photoabsorption cross sections; (b) — Centroid; (c) — FWHM. Dashed lines — zero sound limit. Long-dashed lines — first sound limit.

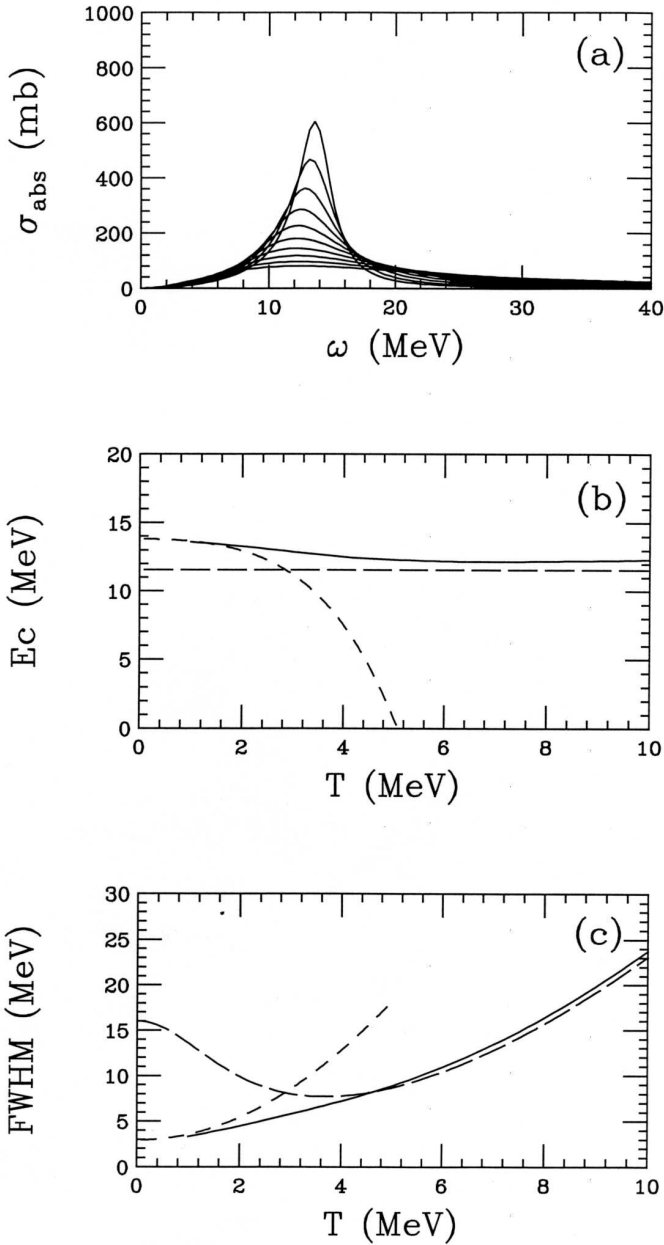


Fig. 2. Temperature dependence of Pb GDR strength distributions for $\tau_2 = \tau_1/3$. Symbols like in Fig. 1.

For the $l = 1$ component, corresponding to an initial shift of the neutron and proton Fermi spheres, we have consistent theoretical estimations [27,28].

Including memory effects in the Landau prescription [16] and angle averaged p - n cross sections, reduced by medium effects, we get

$$\tau_1 \simeq \frac{920}{T^2 + (\hbar\omega_r/2\pi)^2} \text{ fm}/c, \quad (7)$$

τ_2 is more difficult to evaluate. However we can estimate a value smaller than τ_1 : (i) Higher order momentum deformations will lead to a faster equilibration; (ii) Now we have contributions from all nucleon-nucleon collisions while in τ_1 only σ_{pn} is present. Assuming on average $\langle\sigma_{pn}\rangle \sim 2\langle\sigma_{nn,pp}\rangle$ we get from isospin algebra $\tau_1 \simeq 1.8\tau_2$ only.

This point is important since for $\tau_1 < \tau_2$ we will not have the transition to first sound before a full damping of the isovector mode. In Fig. 1 we show results for the case $\tau_2 = \tau_1$ (from Eq. (7)). We report the complete strength function σ_{abs} 1(a), centroid 1(b) and FWHM 1(c) (solid lines), in the temperature interval 1–10 MeV, for the “Pb” k -value. The zero-sound (dashed) and first-sound (long-dashed) limits are also shown. The transition takes place at high temperature, around 7MeV.

In Fig. 2 we report the same analysis in the case $\tau_2 = \tau_1/3$. Now the transition appears around $T = 3$ MeV. We have larger values of FWHM at low temperatures and larger shifts for the centroid energy. This can be also directly seen from the σ_{abs} of Fig. 2(a).

The strength function evaluation of Fig. 2(a), *i.e.* $\tau_1 = \tau_2$ and without first sound transition in the physical region [25], has been recently used in the data analysis of hot ^{120}Sn [7] leading to an overestimation of the GDR photon yield. A reduction of relaxation time using free np cross sections gives a better agreement since it reduces the σ_{abs} form factor. Our results seem to indicate (*cf.* figures 1(a) and 2(a)) that the same effect can be obtained from the transition to first sound mechanism.

3. GDR in fusion dynamics

At low beam energies, just above the threshold, the times involved in the fusion dynamics are, in some cases, long enough to allow the formation of long-living very deformed compound nuclei, close to di-nuclear systems. The effect seems to be ruled by the entrance channel mass-symmetry and the compound nucleus fissility [20,29,30]. As a possibility to observe directly such exotic systems, we discuss the very characteristic features of their GDR γ -decays. Noticeable effects on charged particle emissions, particularly for α particles, are also expected [30].

We perform a microscopic mean field picture of the dynamics based on the solution of the Landau–Vlasov kinetic equation [31]. Since we are considering fusion processes above the Coulomb barrier we are confident that our

semi-classical approach retains a good validity. We have solved the Vlasov equation starting from the test particle method introduced by Gregoire *et al.* [32], where the time evolution of Gaussian phase space wave packets is considered. 50 test particles per nucleon are used, which represents a reasonably good phase space mapping in order to have a fermionic dynamics [33]. The mean field is built from simplified Skyrme forces corresponding to a soft equation of state, see Sect. 2. Surface effects are accounted for within the Gaussian widths. We have considered the systems studied in Ref. [34], but at lower beam energies, *i.e.* the formation of a compound nucleus ^{162}Yb at $E_x \simeq 100$ MeV in two different entrance channels: the mass-asymmetric $^{16}\text{O} + ^{150}\text{Sm}$ at 160 MeV and the mass-symmetric $^{86}\text{Kr} + ^{76}\text{Ge}$ at 258 MeV. In order to have roughly the same angular momentum in the compound system we will compare the dynamics of the impact parameter $b = 5$ fm for the O–Sm reaction to the $b = 3$ fm collision for the Kr–Ge case, so that the spin of the compound system is around $50\hbar$.

In Fig. 3 we show the time evolution of the quadrupole moment for the two reactions. It is possible to observe that in the mass symmetric case the system has still an elongated shape at $1000\text{fm}/c$, while the asymmetric case shows a shape equilibration already at about $200\text{ fm}/c$.

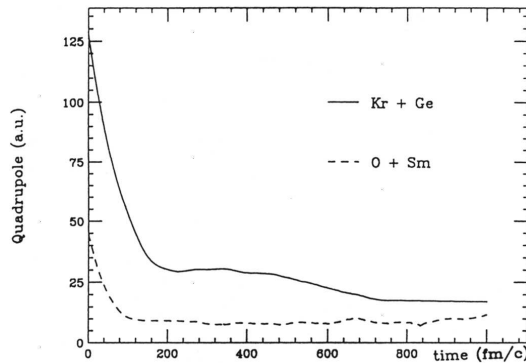


Fig. 3. Time evolution of the quadrupole moment in the Kr–Ge case (full line) and in the mass-asymmetric O–Sm case (dashed line).

In order to follow the dipole dynamics of the whole interacting system, we have evaluated the isovector dipole moment in coordinate space at each time step, choosing the z -direction along the rotating maximum elongation axis and the x -direction on the reaction plane:

$$D_z(t) = \frac{NZ}{A} [\langle z \rangle_{\text{proton}} - \langle z \rangle_{\text{neutron}}], \quad (8)$$

where $\langle z \rangle_{\text{proton}} = \sum_{i=p} z_i/Z$, $\langle z \rangle_{\text{neutron}} = \sum_{i=n} z_i/N$ and the same for the x - and y -components.

The initial dipole moment along the z -axis, if any, becomes zero in less than 200 fm/ c and this can be seen as the time needed for charge equilibration (more discussion on charge asymmetric channels will be presented later in the section). After that we observe the onset of periodic oscillations, the “statistical” giant dipole mode, but in a deformed nuclear system. For mass symmetric reactions it is possible to distinguish two different frequencies, with the smallest one for the parallel component, as expected for a deformed nucleus.

The effect is particularly evident from the Fourier transforms, defined as

$$S_i(\omega) = |F_i(\omega)|, \quad F_i(\omega) = \int_{t_{\min}}^{t_{\max}} dt e^{i\omega t} D_i(t) \quad (9)$$

and plotted in Fig. 4, in the case of the reactions $^{64}\text{Ni} + ^{100}\text{Mo}$ at 237 MeV and $^{16}\text{O} + ^{148}\text{Sm}$ at 83 MeV [35]. In all our calculations we have chosen the interval 200–1000 fm/ c for the $t_{\min} - t_{\max}$ interval to calculate the Fourier transform, following the above discussion about charge equilibration.

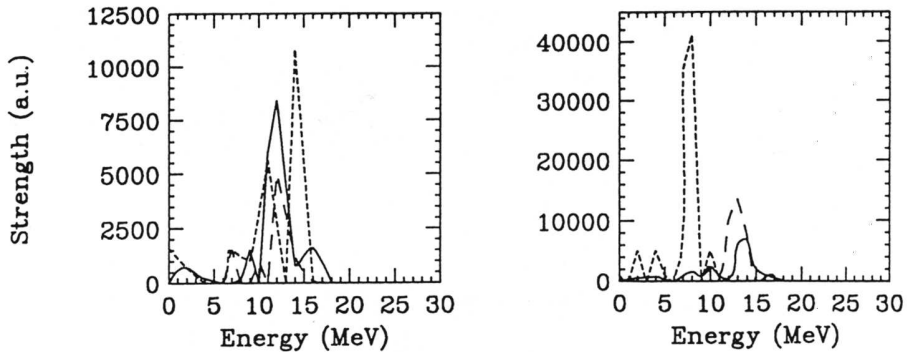


Fig. 4. Fourier transform of the dipole moment components for the collision O–Sm at 83 MeV, $b = 5$ fm (left) and for the collision Ni–Mo at 237 MeV, $b = 3$ fm (right). Dotted line — z component; dashed line — x component; full line — y component (see text). Arbitrary units.

In the more symmetric case the GDR energies associated with the oscillations along the short axes are shifted to larger values, around 14 MeV, for the x -component and the y -component, while the z -component is moved to 7–8 MeV. In the asymmetric case all the components are in the same energy region, 12–13 MeV. So, we can conclude that the system formed in the Ni induced reaction is elongated during a long time. On the other hand, since all the three components are more or less at the same value in the O induced

reaction, it means that the shape becomes spherical or in any case very little deformed in a short time interval.

At this point we can also try to see the differences between the angular distributions of gamma rays coming from the compound systems formed in the two entrance channels. We can directly deduce the expression for the angular anisotropy parameter:

$$a_2 = \frac{\frac{\sigma_y}{2} - \frac{\sigma_z + \sigma_x}{4}}{\sigma_x + \sigma_y + \sigma_z}, \quad \sigma_i = W_i L_i, \quad (10)$$

where W_i is the “shape pre-equilibrium” strength and L_i the Lorentzian function corresponding to the i -GDR component. We remark that in both W_i and L_i terms we have important entrance channel effects, on strengths and frequencies of different oscillation axes. The presence of the deformation has, as a result, a large negative value of the a_2 coefficient in γ -energy regions around 8–10 MeV [29]. This can be used as a trigger for a direct observation of the GDR photons emitted from the intermediate source.

Finally we would like to mention that important information about the early stage of the fusion path can be obtained also studying charge- asymmetric reactions. In fact, in this case it is possible to reveal a “direct” dipole oscillations, related to the charge equilibration dynamics [6, 36, 37].

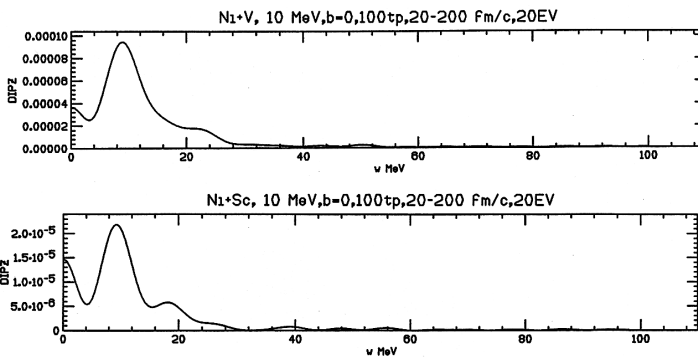


Fig. 5. Fourier transform of the dipole moment z -component for the collision Ni–V at 10 AMeV, $b = 0$ fm (top) and for the collision Ni–Sc at 10 AMeV, $b = 0$ fm (bottom). Arbitrary units.

It is interesting to follow the energy dependence of this effect. We have analysed the two fusion reactions induced by ^{58}Ni ($N/Z = 1.07$) on ^{51}V ($N/Z = 1.22$) and ^{45}Sc ($N/Z = 1.14$) at beam energies 10, 25 and 35 AMeV, central collisions. Although the difference in charge asymmetry is quite small we clearly see the effect on the dynamical dipole. In Fig. 5 we report the Fourier transform of the z -dipole in the first 200 fm/c. In

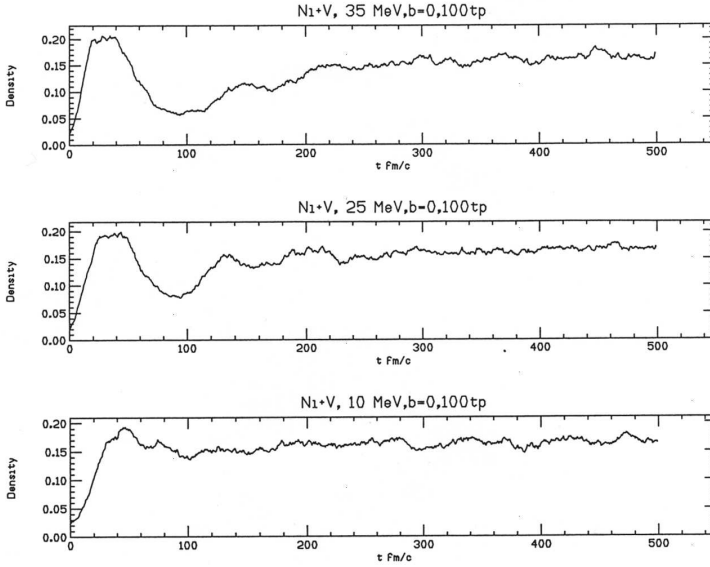


Fig. 6. Density evolution, around c.m., for the collision Ni–V at 10 AMeV, 25 AMeV and 35 AMeV, $b = 0$ fm, from bottom to top.

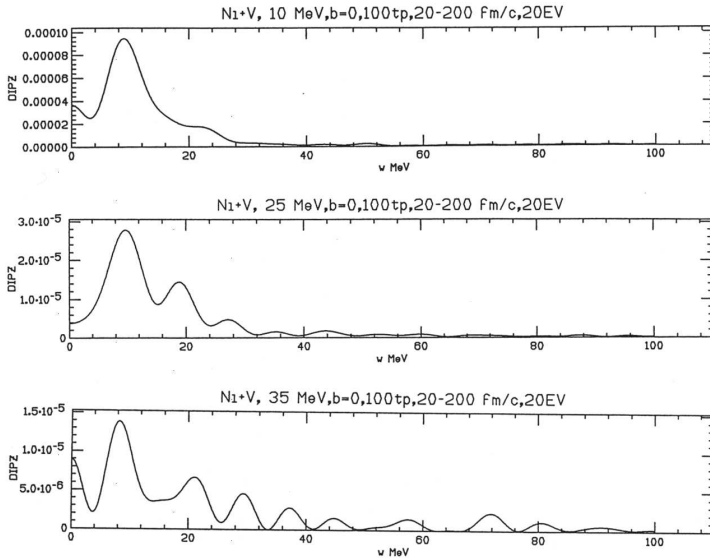


Fig. 7. Fourier transform of the dipole moment z -component for the collision Ni–V at 10 AMeV, 25 AMeV and 35 AMeV, $b = 0$ fm, from top to bottom. Arbitrary units.

both cases we have a nice peak around 8–9 MeV but the strength in the Ni + V case is four times larger. This number roughly corresponds to the ratio of the static dipoles at the touching point. With increasing beam energy the effect is softening for the emission of pre-equilibrium particles and for new dynamical features. In Fig. 6 we show the density evolution around the centre of mass for the Ni + V reaction with increasing beam energy. In the charge equilibration interval 20–200 fm/ c the system goes from normal density (at 10 MeV) to large compression-expansion oscillations at 35 A MeV. As we see from Fig. 7 the dynamical dipole strength is reduced and more fragmented, although still present as confirmed from very recent data [38].

4. Isospin effects: extended Landau dispersion relations

The collective response around the neutron drip line has been studied in a RPA approach [39–41] revealing some interesting new effects: *(i)* A strong coupling between isoscalar and isovector motion; *(ii)* Quite large spreading of the strength in the low frequency region, partially due to threshold contributions from loosely bound neutrons. Here we try to understand these effects, and to make new predictions, in a quite general framework, following a dispersion relation approach for the propagation of collective modes in asymmetric (neutron rich) nuclear matter.

We also show that it could be possible to extract some unique information on the symmetry term of the nuclear EOS in regions away from normal density. We can put then some experimental constraints on the theoretical predictions used in astrophysical contexts [42], where such information is essential in understanding the lives of neutron stars [43–46]. Moreover there are quite stimulating predictions on new phases of asymmetric NM that eventually could be reached during heavy ion reaction dynamics with radioactive beams. The onset of coupled mechanical and chemical instabilities is envisaged [47–49], that should lead to clear experimental signatures.

In the nuclear equation of state we have a symmetry term in the form

$$\frac{E}{A}(\rho, I) = \frac{E}{A}(\rho) + \frac{E_{\text{sym}}}{A}(\rho) I^2 \quad (11)$$

with $I = (N - Z)/A$ asymmetry parameter, given by kinetic and potential contributions

$$\frac{E_{\text{sym}}}{A}(\rho) = \frac{\varepsilon_{\text{F}}(\rho)}{3} + \frac{C(\rho)}{2\rho_0} \rho. \quad (12)$$

In Fig. 8 we report the density dependence of the potential symmetry contribution, second term of Eq. (11), for three different Skyrme effective interactions, SIII, SKM* (Ref. [50]) and Skyrme–Bonn, obtained in order to reproduce the EOS of a microscopic nuclear matter calculation with the

Bonn A potential [49]. While all curves obviously cross at normal density, quite large differences are present in low density and particularly in high density regions.

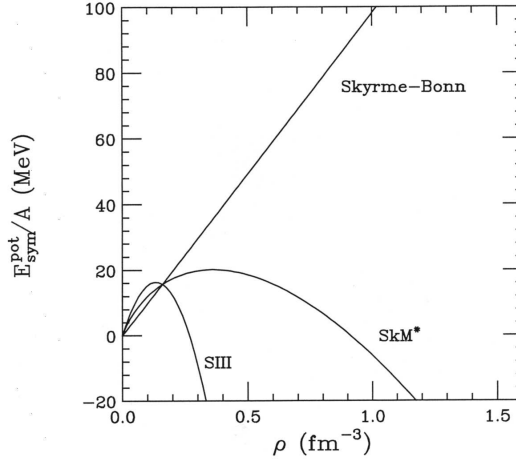


Fig. 8. Density dependence of the potential symmetry term for different Skyrme effective forces.

The Landau dispersion relation approach can be used to study collective modes in asymmetric nuclear matter just starting from the Vlasov kinetic equations of two fluids, neutrons and protons, coupled through the self-consistent mean field [51,52]. Here we will extend the method to regions far from normal density in order to compare predictions of different effective forces. We use the general Skyrme-like form for neutron and proton mean field potentials Eq. (2).

In the variation of the neutron (proton) mean field both isoscalar and isovector density variations will appear:

$$\delta U_q = \alpha_q(\rho_s, \rho_i)\delta\rho_s + \tau_q\beta_q(\rho_s, \rho_i)\delta\rho_i, \quad (13)$$

where

$$\alpha_q = \frac{A}{\rho_0} + (\alpha + 1)B\frac{\rho_s^\alpha}{\rho_0^{\alpha+1}} + \tau_q\frac{\partial C}{\partial\rho_s}\frac{\rho_i}{\rho_0} + \frac{1}{2}\frac{\partial^2 C}{\partial\rho_s^2}\frac{\rho_i^2}{\rho_0},$$

$$\beta_q = \frac{C}{\rho_0} + \tau_q\frac{\partial C}{\partial\rho_s}\frac{\rho_i}{\rho_0}.$$

As a consequence, the linearized Vlasov equations for the isoscalar and isovector variations of the distribution function will also be coupled

[49, 51, 58]. We can derive, using the Landau procedure, a system of coupled equations for the k -component of the isovector and isoscalar density variation and then an extended dispersion relation (d.r.):

$$(1 + F_n^i L_n + F_p^i L_p) (1 + F_n^s L_n + F_p^s L_p) = (F_n^s L_n - F_p^s L_p) (F_n^i L_n - F_p^i L_p), \quad (14)$$

where $F_{n(p)}^s$ and $F_{n(p)}^i$ are the isoscalar and isovector Landau parameters for neutrons (protons):

$$F_{n(p)}^s = \frac{3}{4} \frac{\rho}{\varepsilon_F(\rho)} \frac{p_F^{n(p)}}{p_F} \alpha_{n(p)}, \quad F_{n(p)}^i = \frac{3}{4} \frac{\rho}{\varepsilon_F(\rho)} \frac{p_F^{n(p)}}{p_F} \beta_{n(p)}, \quad (15)$$

$p_F(\rho_s)$ is the Fermi momentum and $L_{n(p)}$ is the Lindhard function associated with the neutron (proton) sound velocity:

$$L_{n(p)} = 1 - \frac{s_{n(p)}}{2} \ln \left(\frac{s_{n(p)} + 1}{s_{n(p)} - 1} \right)$$

with $s_{n(p)} = \omega_k / kv_F^{n(p)}$ being the sound phase velocity in neutron (proton) Fermi velocity units.

In the case of symmetric nuclear matter, we get back to the uncoupled dispersion relation for isoscalar and isovector modes :

$$1 + F_0^s L(s) = 0, \quad 1 + F_0^i L(s) = 0,$$

where $L(s) \equiv L_n = L_p$, $F_0^s \equiv 2F_n^s = 2F_p^s$ and $F_0^i \equiv 2F_n^i = 2F_p^i$ are respectively the Lindhard functions associated with the sound velocity $s = \omega/kv_F$, and the usual isoscalar and isovector Landau parameters [13, 22]:

$$F_0^s = \frac{3}{2} \frac{\partial U}{\partial \rho} \frac{\rho}{\varepsilon_F}, \quad F_0^i = \frac{3}{2} \frac{C}{\rho} \frac{\rho}{\varepsilon_F}. \quad (16)$$

Before discussing the solutions of the new d.r. Eq. (14) it is instructive to make explicit the asymmetry dependence of variables s_n and s_p . Since $\rho_n = \rho(1 + I)/2$, $\rho_p = \rho(1 - I)/2$, we have

$$s_n = s \left(\frac{p_F}{p_F^n} \right) = s \left(\frac{\rho}{2\rho_n} \right)^{1/3} = \frac{s}{(1 + I)^{1/3}},$$

$$s_p = s \left(\frac{p_F}{p_F^p} \right) = \frac{s}{(1 - I)^{1/3}}.$$

These relations are particularly significant. Indeed, corresponding to solutions with $0 < s - 1 \ll 1$ obtained for symmetric matter, in the asymmetric

case we will see a “diving” into the $s_{n,p} < 1$ region, *i.e.* the disappearance of the corresponding collective mode due to Landau damping. Physically it means that with increasing asymmetry the collective mode starts to interact with nucleons of an increasing Fermi sea (with neutrons, if $I > 0$, or protons, if $I < 0$), until completely swallowed .

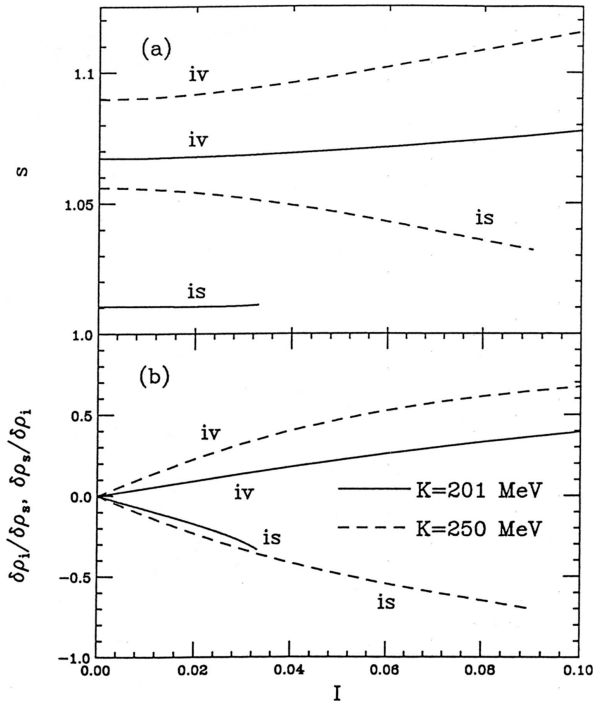


Fig. 9. Velocity s for isovector and isoscalar mode (a) and ratios of densities $\delta\rho_s/\delta\rho_i$ for isovector and $\delta\rho_i/\delta\rho_s$ for isoscalar mode (b) as functions of asymmetry I . Solid lines — SKM, dashed lines — Sk-Bonn.

The above discussion is confirmed solving numerically the new d.r. (14). We have performed calculations with the Skyrme-like effective interactions quoted before. In Fig. 9 we report the solutions s of the d.r. (a) and the corresponding ratio of isoscalar and isovector components (b) for nuclear matter prepared at the density value $\rho = 1.3\rho_0$ ¹ as functions of the asymmetry I for the two forces. Below we will identify the solution with $|\delta\rho_s| > |\delta\rho_i|$ as the isoscalar solution and the one with $|\delta\rho_i| > |\delta\rho_s|$ as the isovector solution.

¹ We choose a slightly higher density, for the discussion of sound mode properties around the normal density value, because for a soft ($K = 201$ MeV) Skyrme interaction the isoscalar mode is already in the region of Landau damping at $\rho = \rho_0$, *i.e.* $-1 < F_0^s(\rho = \rho_0) < 0$.

The solution which has lower sound velocity (the isoscalar one) disappears at small asymmetry, where the corresponding mode has about 40% (for SKM*) or 70% (for Sk-Bonn) of isovector strength. This disappearance does not depend on the choice of the interaction, but only on the relation between Landau parameters at normal density ($F_0^s < F_0^i$) which is always satisfied. Thus, in neutron rich nuclear matter, we expect a general “fragility” of the isoscalar modes, which will enter the Landau overdamped region with loss of collectivity and large spreading of the strength function in the low frequency region [53]. This represents a nice guideline to interpret the results of RPA calculations for neutron drip line nuclei [39–41]. We have, however, to remark that Coulomb, finite size and quantum effects are all acting in the direction of a more robust collective response, which in our results seems to disappear for very low values of the asymmetry parameter.

Some new features can appear at high densities, due to the crossing of the two Landau parameters, predicted by all effective forces. When the density becomes greater than $\rho_{\text{cross}} \simeq 1.4 - 1.5\rho_0$, the isovector mode dives into the overdamped region already at relatively small asymmetries. Indeed at $\rho > \rho_{\text{cross}}$ the velocity of the isovector mode will be now close to the Fermi velocity of neutrons. This will induce a gradual loss of the collectivity, due to the neutron component of the mode.

It is clear that with increasing density we can predict the onset of unstable isovector solutions of the Landau dispersion relations, *i.e.* purely imaginary sound velocities leading to a separation of the neutron and proton fluids [54]. This effect will be closely related to the behaviour of the symmetry term and it will appear only for effective forces which show an attractive symmetry component at high density (like SIII, SKM*). In particular the SIII interaction predicts an isovector instability already at densities $\rho > 2.5\rho_0$ while a force with a monotonic increase of the symmetry term (like the Sk-Bonn) will never reach this instability region.

Now we will focus the attention on more microscopic features of the instabilities in low density asymmetric nuclear matter. This “*Spinodal*” region is particularly important since it can be directly related to the fragment formation mechanism [55–57] and therefore to precise observables in fragmentation reactions with radioactive beams.

From the generalized Landau dispersion relations we get [49, 58]:

1. The region of low density instabilities is shrinking with increasing asymmetry. In a sense this should be expected from the softening of the EOS. As a consequence the growth time $\tau = 1/\Im\omega$ and the most unstable wavelength $\lambda = \frac{2\pi}{k}$ of the instabilities are increasing. Experimentally this effect should show up in a larger size of the primary produced fragments and a reduction of their collective kinetic energy (slower formation, closer to the expansion turning point).

2. The coupling between isoscalar and isovector modes leads to a *chemical* contribution in the instability: we see a larger proton component in the collective density oscillation which gives rise to clusterization.

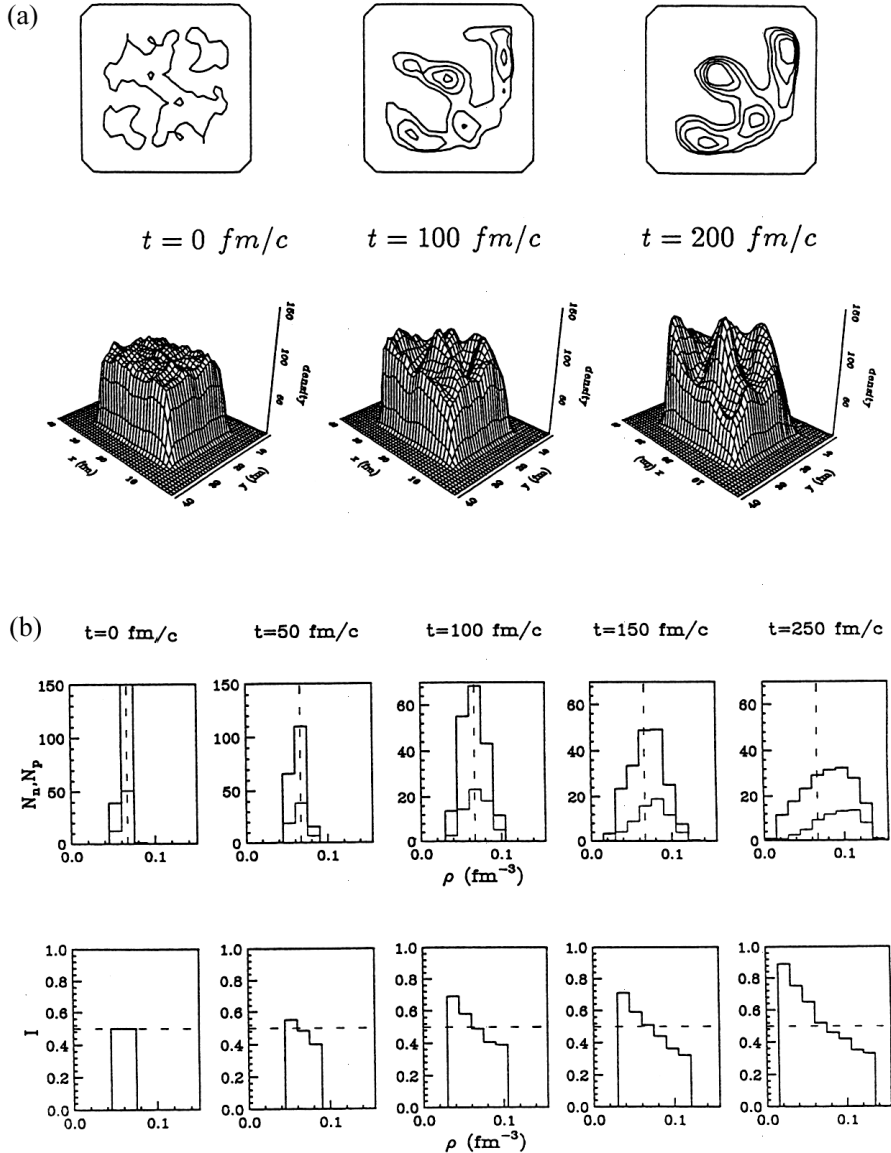


Fig. 10. (a) — density evolution of dilute asymmetric nuclear matter in a box (SKM^* force); (b) — time evolution of neutron, proton and asymmetry distributions in various density bins.

Therefore we have a collective trend towards charge symmetry restoration in the formed fragments. *This is a pure dynamical effects, on short time scales, due to the charge structure of the instability.* The effect is shown in Fig. 10 where (a) density plots of asymmetric NM ($I = 0.5$) in a box of size $L = 8$ fm initially at $\rho = 0.4\rho_0$ are reported (periodic boundary conditions [13, 58]). In (b) we have the time evolution of asymmetry distribution in various density bins. We clearly see the formation of clusters with a quite reduced asymmetry while the surrounding gas is mostly made of neutrons only. The “freeze-out time” will finally fix the proton fraction in the “gas” phase, signature of the low density behaviour of the symmetry term [49, 58], in particular of its *slope*. We remark that the latter is also strongly affecting the diffuseness of the *neutron skin* [59].

5. Summary and perspectives

Hot GDR

After some comments on the open problem of hot nuclei formation we have presented the main features of a transition from zero to first sound for the propagation of the isovector dipole mode. We have shown that the presence of a damping of the isovector current largely influences the transition introducing new effects that are absent in the others, one component, Fermi liquids.

For physical values of the different relaxation times we expect to see the transition at relatively low temperatures in medium-heavy nuclei. In these cases we have shown that the presence of such transition strongly modifies the GDR strength function in a direction consistent with a better agreement with experiments.

GDR and fusion dynamics

Spectra and angular distributions of GDR photons can give direct information on the fusion path in different entrance channel reactions. We remark that the analysis presented here could be used to select the best entrance channel choices for the population of very deformed bands in fast rotating compound nuclei.

Moreover, for charge asymmetric reactions, the “direct” dipole emission could be an interesting cooling mechanism to favour the fusion of very heavy nuclear systems. From the interplay between charge and shape equilibration time-scales we can also suggest new experiments to study the dipole propagation in excited nuclei. In particular the presence of a dynamical dipole enhancement also at higher beam energy, around 20–30 MeV/ u , could bring new independent information on the spreading width of the GDR in very hot

nuclear systems and also on the limits of (*incomplete*) fusion processes. The use of radioactive beams will enhance the possibility of such observations.

Isospin dynamics

For isospin effects on the collective response some simple physical mechanisms are proposed to understand the isoscalar-isovector coupling, the “fragility” of isoscalar modes at normal density and the appearance of new instabilities, all directly related to the properties of the symmetry term. A new chemical component in the spinodal region is expected, with observable signatures on the isotopic content of the dynamically produced fragments. This effect will be enhanced in the overlapping zone of semi-peripheral collisions (the neck region) where the NM asymmetry shall be larger.

We stress the close relation between structure and reaction studies. A possibility is emerging of obtaining in terrestrial accelerator laboratories important information on the symmetry term of great astrophysical interest [46].

REFERENCES

- [1] A. van der Woude, *Nucl. Phys.* **A599**, 393c (1996).
- [2] D.M. Brink, *Nucl. Phys.* **A519**, 3c (1990).
- [3] K.A. Snover, *Annu. Rev. Nucl. Part. Sci.* **36**, 545 (1986).
- [4] J.J. Gaardhoje, *Annu. Rev. Nucl. Part. Sci.* **42**, 483 (1992).
- [5] P.Piattelli, Proc. Giant Resonance Conf., Varenna May 98, *Nucl. Phys.* **A** in press.
- [6] V. Baran *et al.*, *Nucl. Phys.* **A599**, 29c (1996).
- [7] M. Thoennessen, Proc. Giant Resonance Conf., Varenna May 98, *Nucl. Phys.* **A** in press; G. Gervais, M. Thoennessen, W.E Ormand, *On the temperature dependence of the GDR in ^{120}Sn Preprint MSUCL-1099, May 98.*
- [8] M. Kicinska-Habior, *Acta Phys. Pol.* **30**, 1353 (1999).
- [9] Proc. Giant Resonance Conf., Groningen 1996, *Nucl. Phys.* **A599** (1996) issue.
- [10] T. Baumann, E.Ramakrishnan, M. Thoennessen, *Acta Phys. Pol.* **B28**, 197 (1997) and references therein.
- [11] T. Baumann *et al.*, *Nucl. Phys.* **A** in press.
- [12] V.N. Kondratyev, M. Di Toro, *Phys. Rev.* **C53**, 2176 (1996).
- [13] V. Baran *et al.*, *Progr. Part. Nucl. Phys.* **38**, 263 (1997).
- [14] W.R. Abel, A.C. Anderson, J.C. Weathley, *Phys. Rev. Lett.* **17**, 74 (1966).
- [15] L.D. Landau, *Soviet Phys. JETP* **5**, 101 (1957); E.M. Lifshitz, L.P. Pitaevskii, *Physical Kinetics*, Pergamon Press, 1993.
- [16] A.A. Abrikosov, I.M. Khalatnikov, *Rep. Prog. Phys.* **22**, 329 (1959).
- [17] G.F. Bertsch, *Nucl. Phys.* **A249**, 253 (1975); *Z. Phys.* **A289**, 103 (1978).

- [18] J. Wilczynski *et al.*, *Phys. Rev.* **C54**, 325 (1996).
- [19] P. Paul, *Nucl. Phys.* **A630**, 92c (1998).
- [20] V. Baran *et al.*, *J. Phys. G: Nucl. Part. Phys.* **23**, 1341 (1997).
- [21] V.M. Kolomietz, A.B. Larionov, M. Di Toro, *Nucl. Phys.* **A613**, 1 (1997).
- [22] A.B. Migdal, *Theory of Finite Fermi Systems and Applications to Atomic Nuclei*, Interscience, London 1967.
- [23] H. Heiselberg, C.J. Pethick, D.G. Ravenhall, *Ann. Phys. (N.Y.)* **223**, 37 (1993) and references therein.
- [24] F.L. Braghin, D. Vautherin, *Phys. Lett.* **B333**, 289 (1994).
- [25] M. Di Toro, V.M. Kolomietz, A.B. Larionov, *Isvector vibrations in nuclear matter at finite temperature* Proc. Dubna Conf.on Heavy Ions, Sept.97 and sub. *Phys. Rev. C*.
- [26] V. Baran *et al.*, Proc. Giant Resonance Conf., Varenna May 98, *Nucl. Phys.* **A**, in press.
- [27] S. Ayik, D. Boilley, *Phys. Lett.* **B276**, 263 (1992).
- [28] V.M. Kolomietz, V.A. Plujko, S. Shlomo, *Phys. Rev.* **C54**, 3014 (1996) and references therein.
- [29] V. Baran *et al.*, *Nucl. Phys.* **A600**, 111 (1996).
- [30] M. Cabibbo, V. Baran, M. Colonna, M. Di Toro, *Nucl. Phys.* **A637**, 374 (1998).
- [31] G.F. Bertsch, S. Das Gupta, *Phys. Rep.* **160**, 190 (1989).
- [32] A. Bonasera, F. Gulminelli, J. Molitoris, *Phys. Rep.* **243**, 1 (1994) and references therein.
- [33] P.G. Reinhard, E. Suraud *Ann. Phys.* **239**, 216 (1995).
- [34] M. Cinausero *et al.*, *Phys. Lett.* **B383**, 372 (1996).
- [35] M. Thoennessen *et al.*, *Phys. Rev. Lett.* **70**, 4055 (1993).
- [36] Ph. Chomaz, M. Di Toro, A. Smerzi, *Nucl. Phys.* **A563**, 509 (1993).
- [37] S. Flibotte *et al.*, *Phys. Rev. Lett.* **77**, 1448 (1996).
- [38] F. Amorini, TRASMA exp., Ph.D. Thesis LNS Catania 1998.
- [39] I. Hamamoto, H. Sagawa, X.Z. Zhang, *Phys. Rev.* **C55**, 2361 (1997); *Phys. Rev.* **C56**, 3121 (1997); *Nucl. Phys.* **A626**, 669 (1997).
- [40] F. Catara, E. Lanza, M.A. Nagarajan, A. Vitturi, *Nucl. Phys.* **A614**, 86 (1997); *Nucl. Phys.* **A624**, 449 (1997).
- [41] Contributions of G. Colo', E. Lanza, P.G. Reinhard, H. Sagawa, Proc. Giant Resonance Conf., Varenna May 1998, *Nucl. Phys.* **A** in press.
- [42] I. Bombaci, T.T.S. Kuo, U. Lombardo, *Phys. Rep.* **242**, 165 (1994); I. Bombaci, *Phys. Rev.* **C55**, 1 (1997); M. Prakash *et al.*, *Phys. Rep.* **280**, 1 (1997).
- [43] I.M. Irvine, *Neutron Stars*, Oxford Univ. Press, 1978.
- [44] C.J. Pethick, D.G. Ravenhall in *The Lives of Neutron Stars*, Eds M.A. Alpar *et al.*, NATO ASI Series C Vol. 450 (1995) pp. 59–70.

- [45] V.A. Urpin, *The Lives of Neutron Stars*, Eds M.A. Alpar *et al.*, NATO ASI Series C Vol. 450 (1995) pp. 163–166.
- [46] P. Haensel, Contrib. to this Conference.
- [47] H. Mueller, B.D. Serot, *Phys. Rev.* **C52**, 2072 (1995).
- [48] Bao-An Li, C.M. Ko, *Nucl. Phys.* **A618**, 498 (1997).
- [49] M. Colonna, M. Di Toro, A. Larionov *Collective modes in asymmetric nuclear matter*, *Phys. Lett.* **B**, (1998), in press.
- [50] H. Krivine, J. Treiner, O. Bohigas, *Nucl. Phys.* **A336**, 155 (1980).
- [51] P. Haensel, *Nucl. Phys.* **A301**, 53 (1978).
- [52] S. Hernandez *et al.*, *Phys. Lett.* **B413**, 1 (1997).
- [53] D.M. Brink, J.P. da Providencia, *Nucl. Phys.* **A500**, 301 (1981); J.P. da Providencia, *Nucl. Phys.* **A489**, 111 (1988).
- [54] M. Kutschera, *Phys. Lett.* **B340**, 1 (1994).
- [55] M. Colonna, Ph. Chomaz, *Phys. Rev.* **C49**, 1908 (1994).
- [56] M. Colonna, M. Di Toro, A. Guarnera, *Nucl. Phys.* **A589**, 160 (1995).
- [57] M. Colonna *et al.*, Proc. *Critical Phenomena and Collective Observables*, Eds S. Costa *et al.*, World Scientific 1996, p. 369.
- [58] V. Baran, A. Larionov, M. Colonna, M. Di Toro, *Nucl. Phys.* **A632**, 287 (1998).
- [59] H. Sagawa, private communication.